Article

Multifunctional Anatase–Silica Photocatalytic Material for Cements and Concretes

Valeria Strokova [ID], Yulia Ogurtsova *[ID], Ekaterina Gubareva [ID], Sofya Nerovnaya [ID] and Marina Antonenko [ID]

Department of Materials Science and Technology, Construction Engineering Institute, Belgorod State Technological University Named after V.G. Shukhov, 308012 Belgorod, Russia; vvstrokova@gmail.com (V.S.); 43448504@mail.ru (E.G.); nerovnaya.sofya@yandex.ru (S.N.); labuzova326@mail.ru (M.A.)
* Correspondence: ogurcova.yn@bstu.ru

Abstract: The purpose of this research was to study the influence of multifunctional anatase–silica photocatalytic materials (ASPMs) with various photocatalytic and pozzolanic activities on the properties of white portland cement and fine-grained concrete. ASPMs were synthesized by a sol–gel method, during which the levels of photocatalytic and pozzolanic activity were regulated by a certain amount of solvent. ASPMb, obtained with the use of a smaller amount of solvent, was characterized by increased pozzolanic activity due to the lower degree of coating of the surface of diatomite particles with titanium dioxide and the higher content of an opal–cristobalite–tridymite-phase and Bronsted acid sites. They promoted the reaction of diatomite with portlandite of cement stone and allowed significant decreases in the strength of cement–sand mortar to be avoided when replacing 15% of the cement with ASPMs. This allowed self-cleaning fine-grained concrete to be produced, which, after forced carbonization, simulating the natural aging of the product during operation, retained the ability of self-cleaning without changes. ASPMc, produced with the use of a larger amount of solvent with a more uniform distribution of titanium dioxide on the surface of diatomite, allowed fine-grained concrete with a high self-cleaning ability to be obtained, but with a lesser manifestation of the pozzolanic effect.

Keywords: sol–gel synthesis; titanium dioxide; diatomite; photocatalytic activity; pozzolanic activity; cement; hydration; concrete; carbonization; composite material; self-cleaning

1. Introduction

The large-scale introduction of photocatalytic materials into construction will meet a number of requirements for modern building materials and technologies. The first is the use of materials with new properties and materials that ensure environmental safety. The second is the increased use of additives that extend the service life of concrete products and structures. The third is a reduction in the cost of maintenance and periodic servicing owing to the increasing periods between the forced cleaning of surfaces from contamination and restoration [1].

Over time, more and more photocatalytic additives of various compositions have appeared. Therefore, an important research direction is to study their effect on the properties of cement systems and concretes to ensure their large-scale introduction into production and operation.

To date, titanium dioxide has seen significant scientific development and practical applications as a component of photocatalytically active self-cleaning systems. A current research direction is the development of methods for modifying photocatalytic materials based on titanium dioxide, aiming to optimize and increase the efficiency of their functioning [2].

The application of titanium dioxide to substrates with high specific surface areas allows for the following effects: The first is the better distribution of titanium dioxide particles

without their agglomeration [3]. The second is an increase in the volume of simultaneously occurring photocatalytic reactions by increasing the surface area available for the sorption of pollutant molecules and the retention of the photocatalytic decomposition byproducts near the surface of the photocatalyst for their re-involvement in the process [4,5]. The third is better light scattering and absorption, which increases the number of photons interacting with the photocatalytic agent [6]. The fourth is the separation and lower recombination of photogenerated electron–hole pairs [7,8], which increases the efficiency of the photocatalytic decomposition of pollutants. The above-mentioned effects can be fully exploited when photocatalytic agents are evenly distributed over the surface of a substrate.

In the case of the construction industry, as a promising consumer of photocatalytic materials based on nanoscale titanium dioxide due to its features (multi-tonnage production, the possibility of the use of mineral waste, the multicomponent composition and the polystructure of construction composites, and the specific phase and the structure formation of cement systems), the most satisfying way to modify nanoscale titanium dioxide for photocatalytic purposes is deposition onto silica substrates [9]. This is because silica materials are the most widely used active mineral additives in cement composites, allowing cement consumption to be reduced in order to minimize the negative impacts of the cement industry on the environment while maintaining the required strength of composites [10]. The remaining modification methods—for instance, doping—require the use of more expensive, less accessible raw materials, and they are related to fine chemistry, which is economically impractical, considering the volumes and specifics of the production of building materials [11].

Despite significant advances in the synthesis of highly active photocatalysts, there are still open questions regarding attempts to increase the effectiveness of their use in composites, particularly in polymineral and polystructural systems, such as modern cement concretes. The first is the choice of application/injection methods and the provision of equal distributions in the surface layer to ensure access to UV radiation [12]. The second is studying its effect on the phase and structure formation of cement systems [13]. The third is the selection of doses to achieve the best influence on physical and mechanical characteristics and the ability of self-cleaning [14]. Also in question is the influence of environmental effects during operation [15].

Studying the use of photocatalysts in cement materials allowed the following urgent problems to be identified. The first is the difficulty of achieving a uniform distribution of nano- and micro-sized photocatalysts in the concrete mixture [16]. The second is the reduction in the physico-mechanical characteristics of concrete products at high doses of the photocatalyst in their composition [17]. The third is the reduction in the efficiency of photocatalysts when they are mixed with concrete components owing to a decrease in the amount of absorbed light (inhibition of photon transport) and the free surface (inhibition of diffusion of reagents) for photocatalytic reactions [18]. The last problem is the loss of photocatalytic activity in a short time as a result of the carbonization of the surface of the cement material [19].

Summarizing the presented review on the obtainment and the application of photocatalytic composite materials in construction composites allows several urgent tasks, which the present work aims to solve, to be identified. When synthesizing the photocatalytic composite material, it is necessary to control the coating of the diatomite surface with a photocatalytic agent and ensure the uniformity of its distribution. When introducing the composite material, "titanium dioxide–substrate", into a construction composite, it is necessary to ensure the retention of the photocatalyst itself in the surface layer in the poly-granular structure under constant aggressive environmental influence. This may become possible due to chemical (chemical affinity) or physical (developed surface) factors. To fulfill this condition, part of the surface of the silica component must be available for reaction with the hydration products of cement and the provision of pozzolanic effects.

In this regard, we assume that the increased functional characteristics of cement systems with photocatalysts are enabled due to the use of the anatase–silica photocatalytic

material (ASPM), obtained by the sol–gel deposition of TiO_2-sol onto diatomite (acting as a carrier) [20–22], in the case of the controlled degree of coating diatomite surfaces with nanoscale titanium dioxide.

In the technology of cement binders and cement-based composites, diatomite is considered an active mineral additive with pozzolanic activity [23]. This is conditioned by the high content of reactive amorphous silica, capable of interacting with the portlandite of the hydrating portland cement to form stable hydrate phases, thus sealing and strengthening the composite structure.

ASPMs, obtained on the basis of diatomite, may exhibit pozzolanic activity, which will depend on the degree of transformation of the amorphous silica phase during sol–gel synthesis and the degree of "filling" of the surface of diatomite with titanium dioxide neoplasms. In turn, the pozzolanic activity of ASPMs will influence the process of the phase and structure formation of the cement system, and, consequently, the final characteristics of self-cleaning concrete.

The aim of this study was to investigate the influence of multifunctional photocatalytic anatase–silica materials with different levels of photocatalytic and pozzolanic activity on the properties of white portland cement and fine-grained concrete based on it.

For this purpose, multifunctional anatase–silica material with different levels of photocatalytic and pozzolanic activity was synthesized in this work, and its influence on the properties of cement dough, cement stone, and fine-grained concrete was studied.

The combination of photocatalytic activity and the ability to enter into pozzolanic reactions in ASPMs should provide the finished products with the required physical and mechanical characteristics and a high self-cleaning ability, the level of which is maintained during the carbonization of the surface with the use of the products.

2. Materials and Methods

2.1. Raw Materials for Obtaining ASPMs

To obtain ASPMs via the sol–gel method, the following components were used. The first was the precursor of titanium dioxide (technical tetrabutoxytitanium $C_{16}H_{36}O_4Ti$ with a mass fraction of titanium of 15.3% (OOO "PROMKHIMPERM", Perm, Russia)). The second was a solvent (a solution of ethyl alcohol C_2H_2OH with a volume concentration of 95% (ZAO "RFK", Moscow, Russia)). The third was the silica carrier (finely dispersed diatomite powder DIASIL (OOO "Diamiks", Inza, Russia)). The properties of the diatomite powder are shown in Table 1. AEROXIDE® TiO_2 P 25 (Evonik Industries AG, Hanau, Germany) was used as a control photocatalyst.

Table 1. The properties of the diatomite powder.

Parameter Name	Value
Appearance	Fine dry powder from light gray to white
Particle size, μm:	
—average (D50)	10.2
—maximal (D90)	36.9
—minimal (D10)	2.4
Pour density, kg/m^3	350.0
Mass fraction of moisture, %	3.4
Specific surface, m^2/g	11.2
pH of the aqueous extract	7.42

2.2. Raw Materials for Obtaining Cement Stone and Fine-Grained Concrete

The following raw materials were used to obtain cement paste and a concrete mixture with the use of the synthesized multifunctional additive ASPM. The first was the binder, a white ordinary portland cement (WOPC) "CEM I 52.5 R Super White" (Oyak Cement, Adana, Turkey) certified in terms of composition and properties for compliance with the norms and requirements of the European standard "EN 197-1" [24]. By weight, it contains

at least 95% of high-quality white clinker and up to 5% of auxiliary components. The chemical composition of the cement is presented in Table 2. The second is the fine aggregate (white (washed) quartz sand shown in Table 3), whose bulk density in the dry condition is 1500 kg/m^3. The content of pulverized and clay particles is 0.8% and humidity is 2.7%, meeting the requirements of GOST 8736-2014 "Sand for construction works" (AO "Khokholsky sand quarry", Voronezh, Russia [25]). The third is the plasticizing additive Melflux 5581F (BASF Construction Additives, Trostberg, Germany).

Table 2. The chemical composition of WOPC.

The Content of Oxides, Mass. %									
SiO_2	Al_2O_3	Fe_2O_3	CaO	MgO	K_2O	Na_2O	SO_3	TiO_2	Others
15.33	3.84	0.23	74.13	1.73	0.52	0.84	3.01	0.15	0.22

Table 3. The granulometric composition of the fine aggregate.

Sieve Size, mm	1.25	0.63	0.315	0.16	Less than 0.16	Fineness Modulus
Partial residuals, %	2.5	23.0	52.0	17.0	5.5	2.0
Total residuals, %	2.5	25.5	77.5	94.5	100	

2.3. ASPMs Synthesis Technique

The anatase–silica photocatalytic material "SiO_2-TiO_2" was synthesized for the cement system by the sol–gel method in accordance with a methodology developed earlier [20]. The mass ratio of raw materials is shown in Table 4. The amount of solvent was changed to achieve a different degree in terms of coating the diatomite particles with titanium dioxide particles.

Table 4. The mass ratio of raw materials for sol–gel synthesis of ASPMs.

Material	Tetrabutoxytitanium	Ethyl Alcohol	Diatomite
ASPM$_b$	1	3	0.4
ASPM$_c$	1	7	0.4

At the first stage, a 95% solution of ethyl alcohol was added to tetrabutoxytitanium during rapid mixing. At the second stage, diatomite powder was poured into the resulting titanium hydroxide sol during constant stirring on a magnetic stirrer without changing the temperature. The mixing time was 2 h. At the third stage, solvent evaporation was ensured by drying the mixture at a temperature of 115 °C for 12 h, followed by roasting at a temperature of 550 °C for two hours.

2.4. Preparation of Cement Paste, Cement–Sand Mortar and the Concrete Mix

The mixture proportions of cement paste, cement–sand, mortar and concrete are shown in Table 5. For the preparation of cement paste and cement stone samples (without the fine aggregate), we introduced diatomite or ASPMs instead of a part of cement. After preparation, the samples in molds were stored (24 ± 1) h in a bath with a hydraulic shutter, and after unmolding they were stored in a bath with water at a temperature of (20 ± 2) °C until a test age was reached.

Cement–sand mortars were prepared and tested to determine their strength in accordance with EN 196-1 [26].

The preparation of the concrete mix for fine-grained concrete and the production of samples were carried out according to a method similar to the method of preparation of cement–sand mortar mentioned in EN 196-1. The composition of the concrete mixture was developed earlier [27] and included the following measurements (consumption in kg per 1 m^3 of the mixture): cement was 278, ASPMs were 33, sand was 1892, plasticizing additive

was 5.5, and water was 110 (mass ratios of the components are shown in Table 5). After vibration compaction, the samples were placed in a steam-curing chamber and treated according to the following regime. The pre-exposure was performed for 1 h at a temperature of 20 °C; the temperature rise lasted for 1.5 h until a temperature of 60 °C was reached; the isothermal exposure was performed for 2 h at a temperature of 60 °C; and the temperature decrease was 4 h in length, falling to a temperature of 30 °C. The cooling took place in thermos mode for 12 h. Steam curing (SC) was chosen for the production of fine-grained concrete in order to approach the production conditions used when manufacturing the products. Control samples of fine-grained concrete (without ASPMs) were also prepared, as were samples with the control photocatalyst AEROXIDE® TiO$_2$ P 25, in which the mixture of diatomite + AEROXIDE® TiO$_2$ P 25 was used instead of ASPMs (to obtain the same structure and the equal TiO$_2$ content in all samples).

Table 5. The mixture proportions of cement paste, cement–sand mortar, and concrete.

| | Mass Ratio of Raw Materials | | | | | | |
| | Cement Paste | | Cement–Sand Mortar | | Concrete | | |
Raw Material	Control	With Additive	Control	With Additive	Control	With Diatomite + AEROXIDE® TiO$_2$ P 25	With ASPMs
WOPC	1	0.85	1	0.85	1	0.9	0.9
Additive (diatomite or ASPMs)		0.15		0.15		0.06	0.1
Sand			3	3	6	6	6
Plasticizing additive					0.02	0.02	0.02
AEROXIDE® TiO$_2$ P 25						0.04	
Water	0.5	0.5	0.5	0.5	0.35	0.35	0.35

After SC, some of fine-grained concrete samples were subjected to forced carbonization in order to artificially age the surface. To conduct forced carbonization, the samples were placed in a desiccator, connected to a pressure sensor and a pump. Air was pumped out of the desiccator, which was then filled with carbon dioxide up to a pressure of 1 MPa. Carbon dioxide was additionally injected every day to maintain a constant pressure level. When it stopped decreasing, the samples were considered carbonized and were removed from the desiccator.

2.5. Research Methods

To determine chemical and mineral compositions of materials, the following devices were used: the X-ray fluorescence spectrometer of the ARL 9900 WorkStation series (Co-anode) (Thermo Fisher Scientific, Ecublens, Switzerland); and the X-ray diffractometer ARL X'TRA (Cu-anode) (Thermo Fisher Scientific, Ecublens, Switzerland). Microstructure features and the elemental composition of the surface of the materials were studied with the use of the high-resolution scanning electron microscope TESCAN MIRA 3 LMU (Tescan Group, Brno, Czech Republic).

2.5.1. Methods of ASPM Research

Granulometric analysis of powdered materials was performed with the use of the laser particle size analyzer ANALYSETTE 22 NanoTec Plus (Fritsch GmbH, Idar-Oberstein, Germany). The measurement range was 0.01–2100 μm. The total specific surface of the materials was determined by the BET method on the Sorbi-MS device (META, Novosibirsk, Russia), with the use of the nitrogen adsorbate gas and helium carrier gas.

For the indirect assessment of pozzolanic activity of ASPMs, their ability to absorb CaO from a lime solution was determined [28,29]. A solution of calcium hydroxide with a certain initial content of calcium oxide was prepared for the study. A sample of the test material was placed in this solution and mixed on the magnetic stirrer. The calcium oxide content was monitored at regular intervals by titration with 0.05 N of a hydrochloric acid solution. In addition, to assess the activity of the ASPM surface, the content of sites with

proton acidity (Bronsted) was determined with the use of the indicator method [30,31], applying a LEKI SS1207 spectrophotometer (LOIP, Saint Petersburg, Russia). This work uses indicators with values of pKa (the negative decimal logarithm of the acid dissociation constant): +1.3; +2.1; +2.5; +3.46; +6.4.

2.5.2. Methods of Studying the Cement System

The heat release of cement during hydration was determined with the use of the isothermal calorimeter ToniCAL 7338 at a temperature of 20 °C (Toni Technik Baustoffprüfsysteme GmbH, Berlin, Germany). The compressive strength of cement and concrete samples was determined with the use of the hydraulic press known as PGM-500MG4A (SKB Stroypribor, Chelyabinsk, Russia).

2.5.3. The Determination of Photocatalytic Activity and the Self-Cleaning Ability of the Materials

The photocatalytic activity of the materials was determined with the use of the technique for evaluating the photocatalytic decomposition of organic dye (rhodamine B (Rhodamine B, $C_{28}H_{31}ClN_2O_3$, Vekton, Saint Petersburg, Russia), adapted earlier from the UNI 11259 standard [32]. The dye solution was applied to the samples at a concentration of 4×10^{-4} mole/L. Then, they were exposed to ultraviolet radiation (UV-A, 1.1 ± 0.1 W/m^2) for 4 and 26 h. Photocatalytic activity (self-cleaning ability) was calculated based on data about the change in the color of the surface of the samples (change in the a* coordinate of the Lab color space) after radiation with the use of the GIMP software (GIMP 2.10.8, Spencer Kimball and Peter Mattis, USA) [20].

Before conducting the study, ASPM powders were pressed into tablets with KBr as a carrier. The amount of the tested powder in the resulting tablet was varied in order to obtain the same TiO$_2$ content in all samples (SiO$_2$ for diatomite).

Cement stone samples with an age of 28 days were examined and produced according to the procedure described in Section 2.4.

After heat and moisture treatment and after steam curing, followed by forced carbonization, samples of fine-grained concrete were examined. They were manufactured according to the procedure provided in Section 2.4.

To assess the self-cleaning ability of fine-grained concrete, an additional method was used to determine a change in the contact angle of wetting in accordance with State Standard of Russia GOST R 57255−2016, entitled "Photocatalytically active self-cleaning concretes. Technical specifications" [33]. The contact angle of wetting was determined with the use of the Kruss DSA 30 device (Kruss GmbH, Hamburg, Germany). This method is based on measuring the change in the contact angle of wetting on the surface of a concrete sample of 100 cm^2 in size, exposed to ultraviolet radiation. Oleic acid was applied to the samples, and the initial contact angle of wetting was measured. The samples were then exposed to ultraviolet radiation (UV-A, 20 ± 1 W/m^2) and the contact angle of wetting was determined every 4 h. Starting from the third measurement, the variation coefficients of the contact angle of wetting K were calculated:

$$K = \frac{s}{\overline{x}} \leq 10\%, \tag{1}$$

where s is the standard deviation of the measurement results at three consecutive points, °; and $\overline{x}$ is the average value of the measurement results of the contact angle of wetting at three consecutive points, °, calculated by the formula:

$$\overline{x} = \frac{(\theta_{n_1} + \theta_{n_2} + \theta_{n_3})}{3}, \tag{2}$$

where $\theta_{n_1}, \theta_{n_2}, \theta_{n_3}$ are contact angles of wetting after n_1, n_2, n_3 h of exposure, respectively, °. The test was completed when the values of the coefficients of variation became lower than 10%.

3. Results and Discussions

### 3.1. The Properties of the Anatase–Silica Photocatalytic Material

The first stage of the study was establishing the influence of the amount of solvent used during sol–gel synthesis of anatase–silica material on its physico-chemical properties and structure.

According to the results of determining the chemical composition of synthesized ASPMs (Table 6), the SiO_2/TiO_2 ratio was about 1.5/1.

Table 6. The chemical composition of the initial diatomite and synthesized ASPMs.

Material	The Content of Oxides, Mass. %									
	SiO_2	TiO_2	Al_2O_3	Fe_2O_3	MgO	Na_2O	K_2O	CaO	SO_3	Others
Diatomite	86.81	0.28	5.91	2.67	2.35	0.34	1.12	0.41	0.01	0.01
$ASPM_b$	56.24	37.31	2.89	1.13	0.52	0.47	0.50	0.21	0.26	0.47
$ASPM_c$	55.53	38.13	2.62	1.18	0.61	0.59	0.51	0.21	0.28	0.34

The analysis of diffraction patterns (Figure 1) shows that in all samples with an additive diffraction profile of the opal–cristobalite–tridymite (OCT) phase, quartz reflections are related to the initial diatomite. In addition, single-phase titanium dioxide with the anatase–crystal structure is present in ASPM samples. In ASPMc (with the higher solvent content during sol–gel synthesis), the intensity of quartz reflections and the area of the region, related to OCT, are lower than the intensity and the area in ASPMb (with the lower solvent content during sol–gel synthesis). This may be conditioned by the more uniform and extensive coating of titanium dioxide particles onto the surface of diatomite in ASPMc and may lead to a decrease in its pozzolanic activity in the cement system.
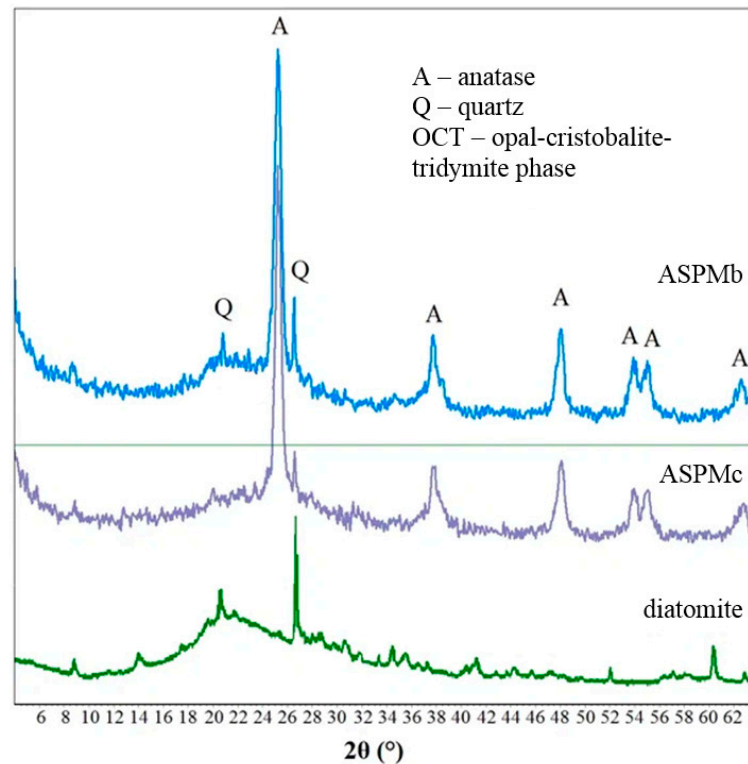
Figure 1. Diffraction patterns of the initial diatomite and synthesized ASPMs.

The microstructure of ASPMs (Figure 2) is characterized by the presence of agglomerates of spherical titanium dioxide particles, appearing both on the surface of diatomite particles and separately. The size of individual TiO_2 particles is 50–150 nm. Accumulations

of nanoscale anatase are observed on diatomite particles with developed amorphous surfaces. At the same time, crystallized particles of diatomite with smooth surfaces remain uncoated by neoplasms of titanium dioxide.
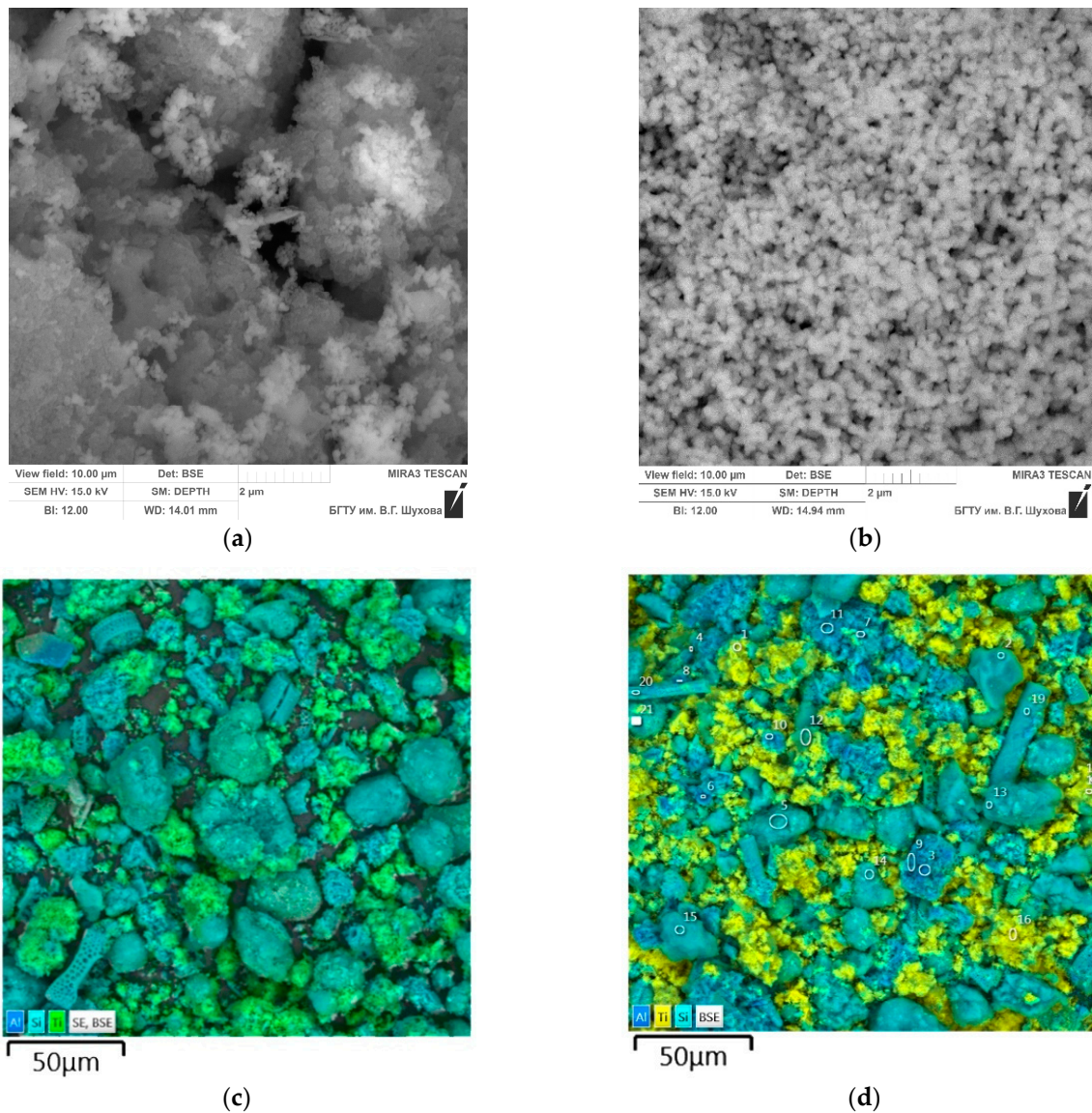
Figure 2. The morphology of ASPMb (**a**,**c**) and ASPMc (**b**,**d**).

According to the results of mapping the microstructures of powders comprising the chemical elements of Si and Ti, in ASPMb (Figure 2c), the coating of diatomite particles with titanium dioxide is dotted, while in ASPMc (Figure 2d), the coated areas of the diatomite surface are coarser, more numerous, and more evenly distributed.

According to the granulometric composition (Figure 3), ASPMc is more homogeneous; it contains particles with dimensions of 0.01 μm and 0.09–106.9 μm, the peak of which is 31.53 μm. The increase in the proportion of large-sized particles for ASPMb samples (0.01, 0.09–154.1 μm, maximum of 58.4 μm) indicates the flocculation of synthesized titanium dioxide, leading to the adhesion of silica particles to each other. The compositions with the increased solvent content (ASPMc) are less susceptible to this process and, at the same time, the non-interacting anatase particles remain in the form of separate fractions.
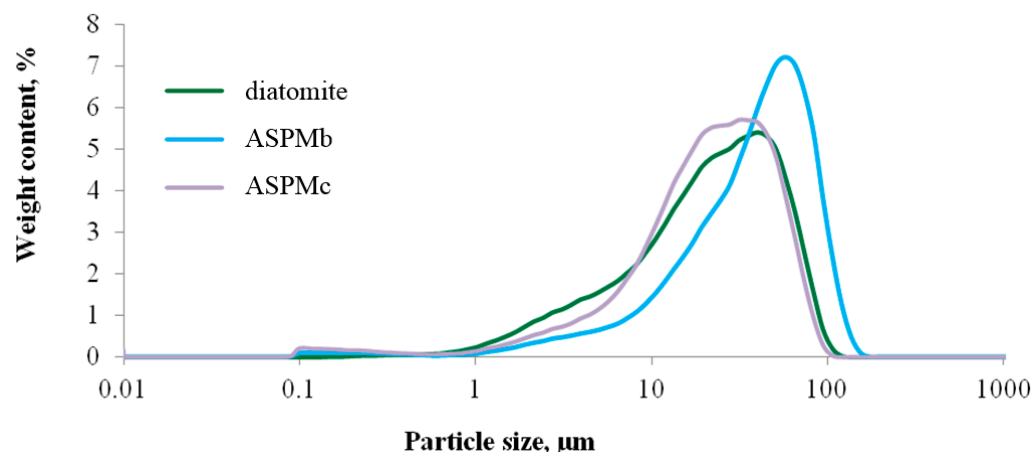
Figure 3. The granulometric composition of the initial diatomite and synthesized ASPMs.

The specific surface of ASPMc (Table 7) significantly exceeds the specific surface of initial diatomite owing to the formation of nanoscale newgrowths of titanium dioxide (see Figure 2b). The specific surface of ASPMb also exceeds that of diatomite, despite some particle enlargement, according to the granulometric analysis (see Figure 3). In this case, the formed nanosized newgrowths of titanium dioxide also contribute to increases in the specific surface area.

Table 7. The properties of the initial diatomite and synthesized ASPMs.

Properties	Materials		
	Diatomite	**ASPMb**	**ASPMc**
Specific surface according to BET, m^2/kg	62,100	63,900	70,400
Sum of Bronsted acid sites, 10^3 mole/g	105.47	62.3	31.47
Photocatalytic activity, %			
—4 h later	12	51	60
—26 h later	14 [1]	86	89

[1] Bleaching as a result of sorption and drying processes.

The study of the absorption of CaO from a lime solution as an indirect characteristic of the pozzolanic activity of materials showed the largest increase in the CaO absorption of all samples in the first hour of the experiment; then, the absorption rate decreased by 30 h (Figure 4). The absorption process of CaO of ASPMb was most similar to the absorption process of diatomite. The slight slowdown was potentially due to the point presence of TiO_2 particles on the surface of diatomite. ASPMc showed reduced pozzolanic activity over the studied period of time and was conditioned by a significant overlap of the diatomite surface with particles and conglomerates of titanium dioxide.

Another property of ASPMs that determines their pozzolanic and photocatalytic activity is the acid–base characteristic of the surface. The purpose of studying Bronsted acid sites (0 < pKa < 7) (Table 7) is because the increase in acidity partially causes an increase in the activity of photocatalytic reactions [34] and redox processes, occurring during hydration and the hardening of cement [35].

After the synthesis of ASPMs, the total concentration of Bronsted acid sites decreases compared to the concentration of initial diatomite, suggesting that the reaction between ≡SiOH (≡SiOR) and ≡TiOH (≡TiOR) proceeds during synthesis, blocking the sites of the carrier surface with titanium dioxide particles. With almost the same chemical and mineral composition of ASPMb and ASPMc, a significant difference in the total concentration of Bronsted acid sites may be conditioned based on particle size and porosity, which may be expressed by the redistribution of donor–acceptor sites, for example, towards Lewis acid sites [36,37].
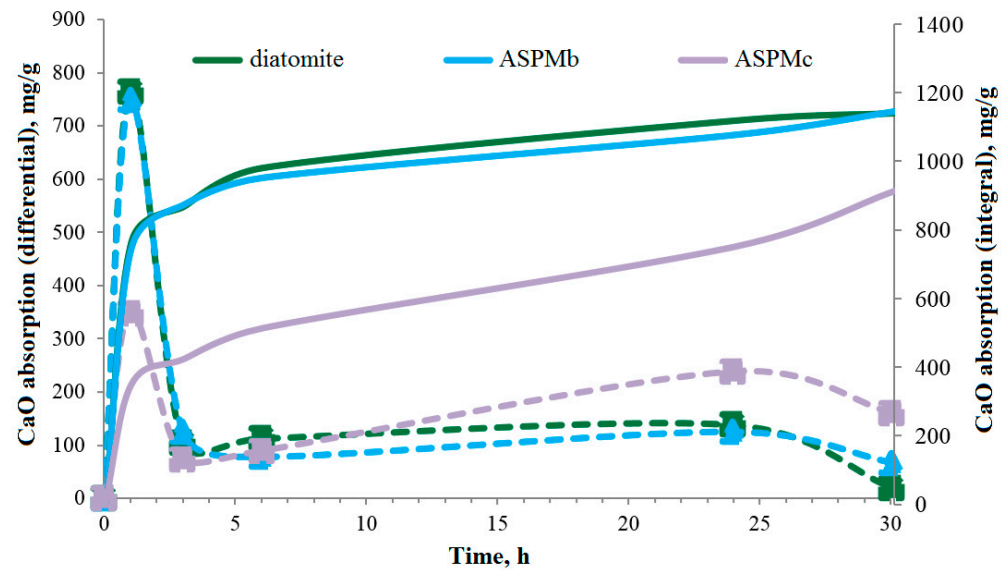
Figure 4. The absorption of CaO from lime solution of 1 g of the studied material: (—)—integral, (- -)—differential.

Both synthesized ASPMs have high photocatalytic activity (see Table 7). After both 4 and 26 h of ultraviolet irradiation, ASPMc has greater ability in terms of self-cleaning. This result is expected and is supported by the results of studying its composition, morphostructural characteristics, and physico-chemical properties. In particular, this is due to the more uniform coating of the diatomite surface with nanosized titanium dioxide from anatase modification and the greater development of its surface. Slightly lower photocatalytic activity of the ASPMb sample may be induced by the presence of TiO_2 conglomerates, its uneven and insufficient distribution on the surface of diatomite particles, and the volume of the composite material. Therefore, when comparing ASPMb and ASPMc, the former shows greater pozzolanic activity, and the latter demonstrates greater photocatalytic activity.

3.2. The properties of the Cement System with the Multifunctional Anatase–Silica Additive

The second stage of the study evaluated changes in the properties of cement paste and stone in relation to the physico-chemical properties and structure of ASPMb and ASPMc.

The study of the heat release of cement paste with additives (Figure 5) showed that all the obtained heat–release curves had similar natures and corresponded to the traditional ones for portland cement. The first peak (the initial hydration phase), occurring at 4–6 min, is associated with the process of exothermic wetting, as well as with early-stage reactions that lead to the formation of gelatin coating and Aft-phase rods [38].

The second peak in the diagram is the main peak of heat release (a middle stage of hydration), corresponding to the hydration of silicates with the formation of C–S–H and CH phases. The subsequent pronounced peak, which is traditionally responsible for the formation of ettringite, is not observed. After the main peak, a shoulder is noted, which can be attributed to the formation of ettringite and to the transition from AFt to the AFm phase or to C_3A hydration with the formation of the AFm phase.

The white portland cement used was fast-hardening, and so the main peak of heat release was observed earlier, 4 h after sealing with water, while it usually occurs at 8–10 h.

Comparing the obtained curves shows that, in the case of the white portland cement without additives, the main peak occurs at 4 h and 30 min from the beginning of the experiment. The times with certain additions are as follows:

- 15% of diatomite—3 h 55 min;
- 15% of ASPMb—3 h 57 min;
- 15% of ASPMc—3 h 48 min.

Some of the shift in the main peak of heat release in the presence of additives may be due to accelerated heterogeneous nucleation of hydrates on the particles of inert materials. In this case, the acceleration of nucleation is associated with a decrease in the energy barrier [39].
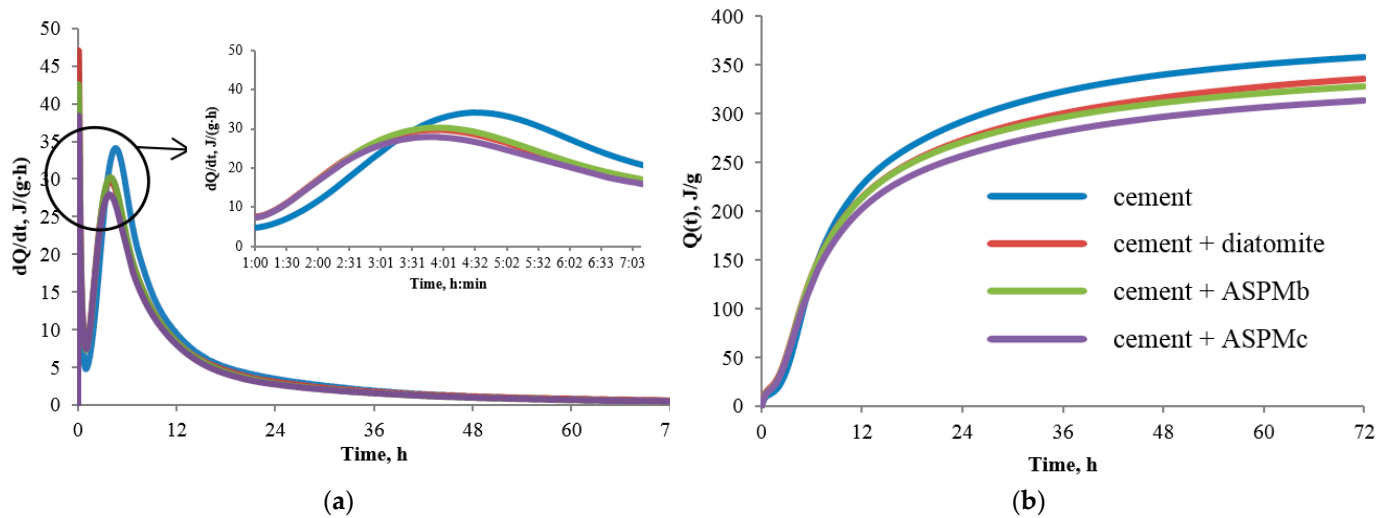
Figure 5. Differential (**a**) and integral (**b**) heat release curves during cement hydration in the presence of various additives.

However, despite the acceleration of the appearance of the main peak of hydration, one can note a decrease in the intensity of the heat release of formulations with additives, relative to the control. This is determined by a decrease in the content of portland cement in the mixture and a change in the amount of the liquid phase (on the one hand, the water–cement ratio increases with the introduction of 15% of the additive instead of part of the cement; on the other hand, the used additives sorb water).

The total amount of heat is an indicator of the number of clinker phases that have reacted over a given period of time.

The total heat released during the hydration of all the studied formulations with additives is noted to decrease in comparison to the control sample after 4 h from the beginning of the experiment. First of all, as already mentioned, this is conditioned by a decrease in the amount of the cement component. However, during the same reduction in the cement consumption, the total amount of released heat differs for different additives and can be ranked by degree of reduction:

diatomite → ASPMb → ASPMc.

Due to the constancy of the conditions, such as the temperature of the system, the particle size, and the amount of cement used, in the case of the materials under study, the total heat released may be influenced by the amount of water in the system. This happens because the sorption capacity of the materials is different; in particular, the ASPMc has the largest specific surface, which means it can hold more water.

Therefore, according to the results of determining the heat release of the white portland cement with additives (diatomite, AEROXIDE® TiO_2 P 25, ASPMb, ASPMc), in the first minutes of hydration, when mineral components are introduced, intense heat release is noted to occur as a result of their wetting. Subsequently, there is a decrease in the intensity of the main peak of hydration and the total heat release of the systems due to a decrease in the proportion of cement. The use of additives slightly accelerates the beginning of the period of active hydration. This may happen because the absorption of part of the water by the mineral component at the initial stages accelerates the process of saturation of a medium with Ca^{2+} ions, and, consequently, the transition from induction to the main hydration period [40]. In addition, mineral additives can act as seeding agents for the

crystallization of $Ca(OH)_2$, as well as participate in the formation of C–S–H phases as a pozzolanic component.

The decrease in the compressive strength of cement stone samples with additives (Figure 6) is primarily due to a 15% decrease in the content of the portland cement in the mixture compared with the control composition. Starting from the 7th day of hardening, there is an excess of the strength values of the composition with diatomite, which may be the result of the pozzolanic reaction. By the 28th day of hardening, the excess is 13.5%. Samples with ASPMb and ASPMc have lower strength than the control and diatomite samples, which is determined by the closure of the reactively active surface of the silica component by anatase particles. The presence of titanium dioxide in compositions with 15% of ASPMb and 15% of ASPMc probably hinders the processes of structure formation and reduces the influence of the pozzolaic effect. By 28 days, the strength compared with the strength of control additive-free cement stone decreases by 10.4% in ASPMb and 11.9% in ASPMc.
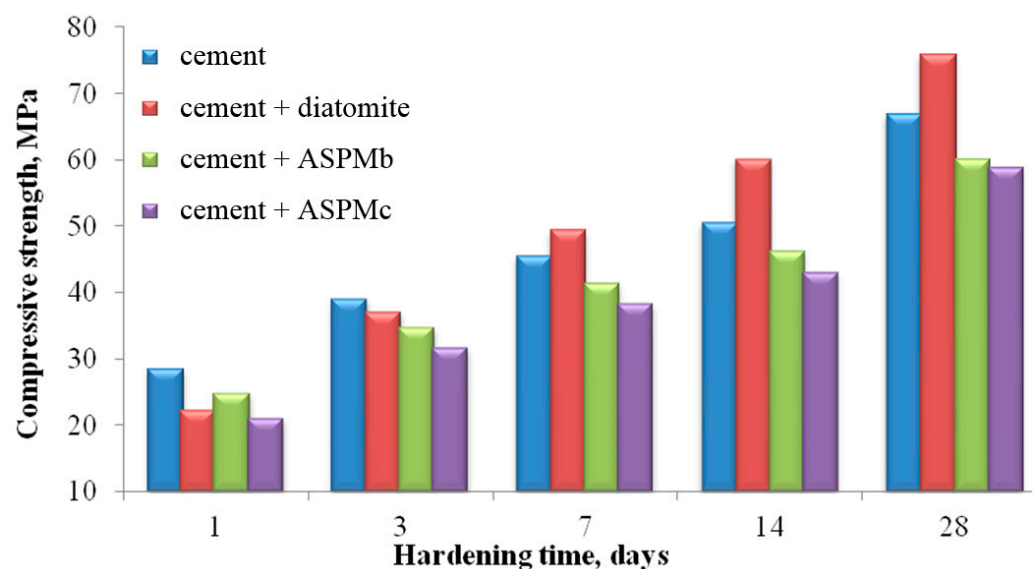
Figure 6. Kinetics of the compressive strength of cement stone depending on the type of additive over time.

According to the results of qualitative X-ray diffraction (Figure 7), the phase composition of all samples is similar. There are reflections of unreacted clinker minerals and hydration products: portlandite and ettringite. In the compositions with additives, a decrease in the intensity of portlandite peaks is observed, which may be related both to the decrease in the content of portland cement in the mixture and to pozzolanic reactions. The comparison of the intensity of the peaks of clinker minerals shows that hydration proceeds at a higher rate in the presence of ASPMb and ASPMc.

The microstructure of cement stone with additives (Figure 8) is visually characterized by the lower content of portlandite crystals and the presence of numerous elongated needle-shaped and fibrous crystals. They are most pronounced in cement stone with diatomite and are less pronounced in cement stone with ASPMc. The morphological difference between newgrowths and non-additive cement stone indicates the formation of these newgrowths owing to the presence of a large amount of free SiO_2 in the composition of the additive. The polymorphostructural nature of such newgrowths can contribute to the formation of composite structures at the nano and micro levels, a reduction in porosity, and an increase in the strength of the conglomerate.
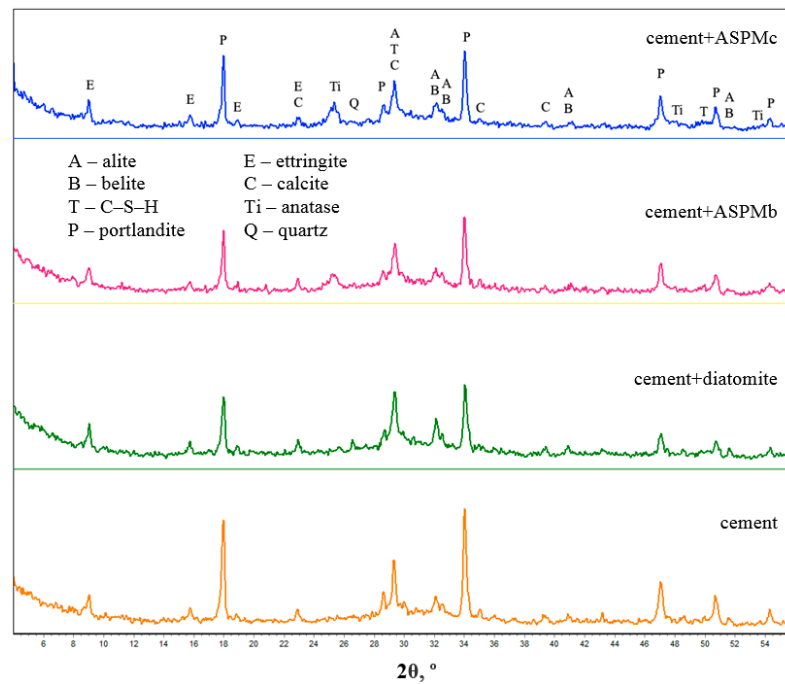
Figure 7. X-ray diffraction patterns of cement stone at the age of 28 days of hardening.
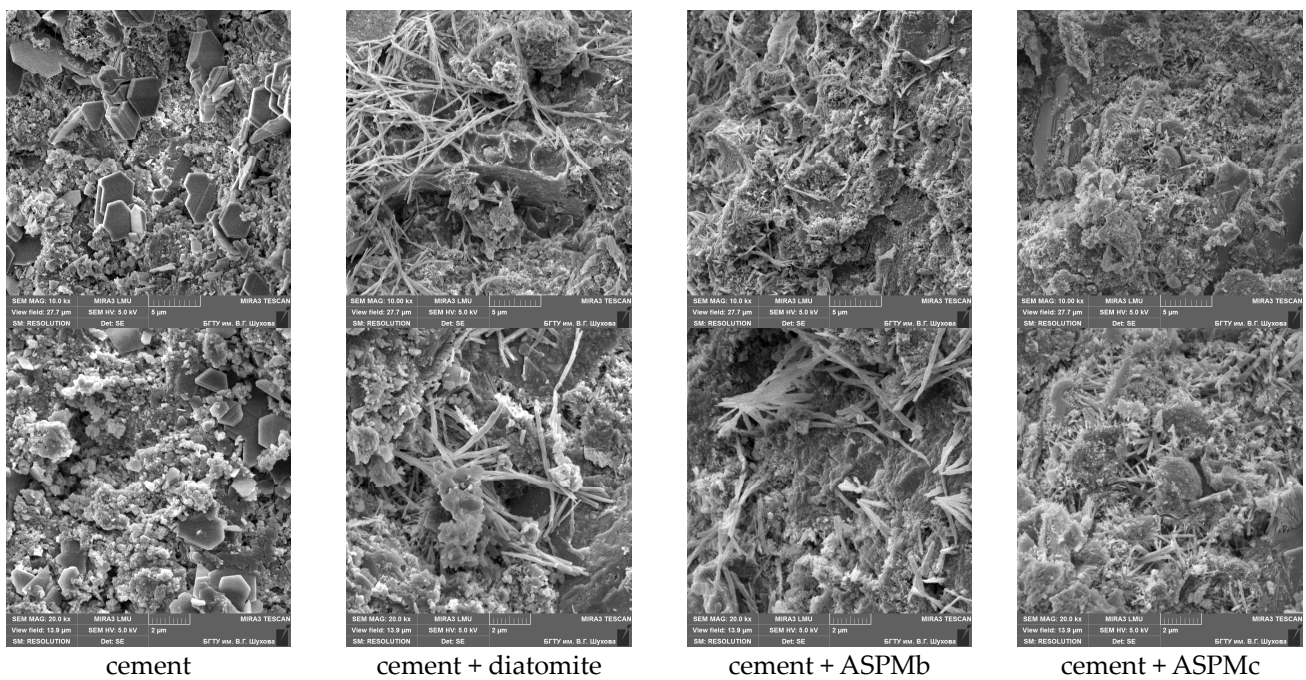
Figure 8. The microstructure of samples after 28 days of hardening.

The results of the study of the self-cleaning ability of cement stone (Figure 9) show the effectiveness of using ASPM additives in the cement system. As a result of sorption and drying, under the influence of ultraviolet radiation, there was a slight removal of rhodamine B from the surface of pure cement stone and cement stone with diatomite. Comparing the two types of ASPMs, one can note the best result for ASPMc: with the use of it, there was an intensive removal of rhodamine B from the surface of cement stone, with a 51.07% presence after 4 h of UV radiation and 71.66% after 26 h.
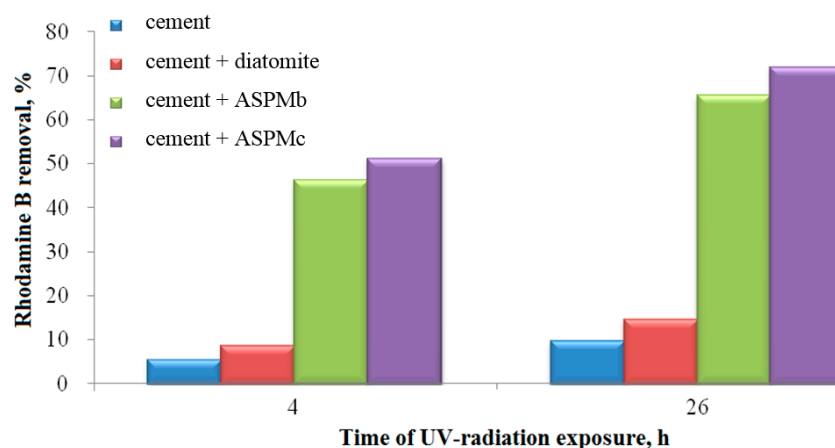
Figure 9. Self-cleaning ability of cement stone samples.

The results of determining the compressive strength of cement–sand mortar with ASPMs (Table 8) at the age of 28 days demonstrate that, in the presence of the fine aggregate, replacing 15% of the cement with ASPMb leads to a decrease in the strength by 9% compared with the strength of the control sample. With the use of ASPMc, the strength is lower by 14% compared to the additive-free control sample and by 7% compared to ASPMb, because this additive is characterized by a more uniform distribution of the photocatalytic agent on the surface of the diatomite (which provides higher values for photocatalytic activity) and, as a result, reduced pozzolanic activity. The strength values for the 28th day are not final because the pozzolanic reaction continues in the longer term.

Table 8. The strength of cement–sand mortar.

Binding	Compressive Strength, MPa
White ordinary portland cement (WOPC)	59.8
85% of WOPC + 15% of ASPMb	54.7
85% of WOPC + 15% of ASPMc	51.0

Nevertheless, the achieved strength indicators allow these mixtures to be recommended for use in the production of fine-grained concrete based on their application in the upper layer of facing concrete products in order to obtain architecturally expressive white and colored surfaces and to reduce the consumption of white cement.

Therefore, comparing the properties of cement stone with ASPMb and ASPMc, the conclusion made in Section 3.1 is confirmed, as ASPMb has greater pozzolanic activity and ASPMc has greater photocatalytic activity.

3.3. The Self-Cleaning Ability of Fine-Grained Concrete with the Multifunctional Anatase–Silica Additive

The third stage of the study was focused on evaluating the influence of the photocatalytic and pozzolanic activity of multifunctional additives of ASPMb and ASPMc on the ability of fine-grained concrete to self-clean, especially after forced carbonation, in order to simulate the natural aging of the product. The compositions and technology required for obtaining concrete, studied in this part of the work, were approximated to industrial conditions.

During the exploitation of concrete products, the photocatalytic decomposition of organic pollutants occurs on the surface of fine-grained concrete with a photocatalytic component (Figure 10) under the influence of ultraviolet radiation. During the operation of structures, concrete carbonization (an interaction of portlandite and C–S–H phases with the CO_2 of air in the presence of moisture) leads to a change in the number of parameters of concrete stone, such as the phase composition, pH, porosity, and the specific active

surface. This, in turn, can reduce the self-cleaning ability of the surface of photocatalytic concrete owing to the shielding effect of carbonization products on photocatalyst particles and the decrease in surface porosity. One of the expected effects of the presence of ASPMs on the composition of concrete is a decrease in the intensity of the carbonization process and its effect on the composition and structure of concrete stone due to the binding of portlandite with amorphous silica diatomite. This should reduce the negative impacts of the carbonization process on the self-cleaning ability of products. In this regard, in the case of fine-grained concrete with ASPMs, which is recommended for the upper front layer of products, the effectiveness of the self-cleaning ability was determined both in its natural state after heat and moisture treatment and after artificial aging (forced carbonization).
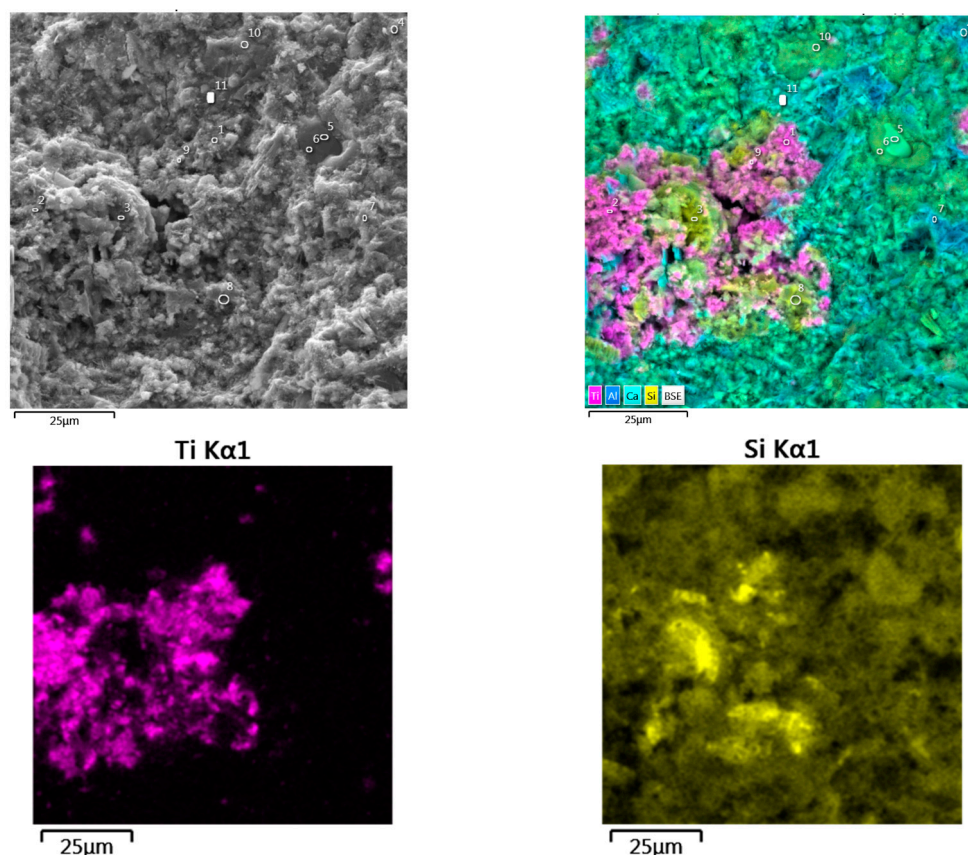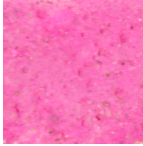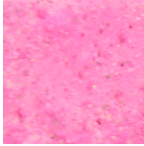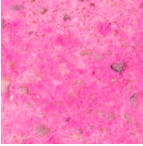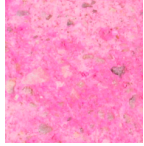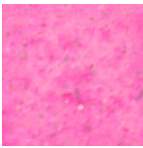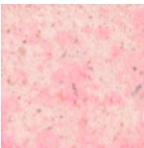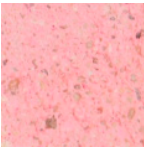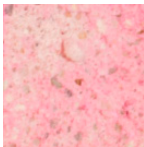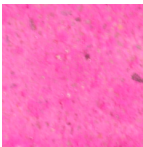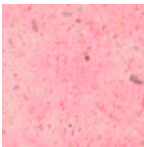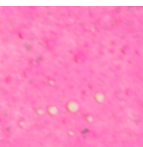
Figure 10. Mapping the surface of fine-grained concrete with ASPMs.

According to the results from determining the self-cleaning ability of concrete with the control photocatalyst (AEROXIDE® TiO$_2$ P 25) and ASPMs (Tables 9 and 10), there was a decrease in the efficiency of removing rhodamine B in all samples when they were subjected to forced carbonization after SC. This was associated with the shielding of the photocatalytically active surface with calcium carbonates. Therefore, in concrete with the control photocatalyst, after 26 h of ultraviolet radiation, the removal of rhodamine B decreased to 58.62% as compared with the value of 70.18% in the sample without carbonization.

The effect of a reduction in self-cleaning ability after carbonization is much less pronounced in fine-grained concrete with ASPMb, which may be determined by the decrease in the content of portlandite as a source of calcium carbonate formation when interacting with CO$_2$ in the air. Concrete containing ASPMc showed greater self-cleaning ability than concrete with ASPMb due to the more uniform distribution of anatase, but the pozzolanic effect was less pronounced in it, which also influenced the decrease in self-cleaning efficiency after carbonization from 64.17% to 61.94%. By the time the final value of the contact angle of wetting was reached on the surface of concrete samples contaminated with oleic acid (Table 10), the results correlated with the results of the rhodamine B removal.

Concrete with ASPMc exhibited a self-cleaning ability, which was closer to the ability of the sample with the control photocatalyst, but concrete with ASPMb retained its self-cleaning ability after forced carbonization much better than others did.

Table 9. The ability of the self-cleaning of fine-grained concrete, determined by the method of evaluating the photocatalytic decomposition of organic dye of rhodamine B.

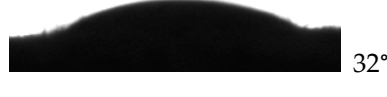| After Steam Curing (SC)		After SC and Carbonization	
Before Radiation	**After Radiation**	**Before Radiation**	**After Radiation**
Fine-grained concrete without additives			
Fine-grained concrete with AEROXIDE® TiO$_2$ P 25			
Fine-grained concrete with ASPMb			
Fine-grained concrete with ASPMc			
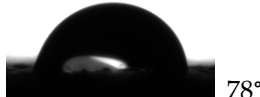
Table 10. The ability of the self-cleaning of fine-grained concrete.

Sample Type	Removal of Rhodamine B after 26 h of UV Irradiation, %		Time to Reach the Final Contact Angle of wetting (GOST R 57255), h [1]	
	After SC	**After SC and Carbonization**	**After SC**	**After SC and Carbonization**
Without additives	15.88	15.81	contact angle of wetting is not reduced	
With AEROXIDE® TiO$_2$ P 25	70.18	58.62	48	60
With ASPMb	57.92	57.09	56	56
With ASPMc	64.17	61.94	52	56

[1] A measurement interval was 4 h.

As a result of the photocatalytic removal of oleic acid from the surface of all the studied samples with additives, the final values of the contact angle of wetting practically reached the values for the initial uncontaminated samples (Table 11). Concrete made with the control photocatalyst required 60 h of UV radiation; concrete made with ASPMs of both types required 56 h (see Table 10).

Table 11. Changing the contact angle of wetting on the surface of fine-grained concretes subjected to carbonization (the method according to GOST R 57255-2016).

Type of Sample, Contact Angle of Wetting before Applying Oleic Acid	Initial Contact Angle of Wetting (after Applying Oleic Acid)	Final Contact Angle of Wetting
Without additives, 31°	79°	78°
With AEROXIDE® TiO$_2$ P 25, 24°	64°	25°
With ASPMb, 32°	82°	35°
With ASPMc, 30°	75°	32°

In view of this, ASPMc, during the sol–gel synthesis of which more solvent was used and which demonstrated greater photocatalytic activity, allows concrete with greater self-purification ability to be obtained, similar to concrete with the control photocatalyst, which exceeds the ability of the control sample after forced carbonation. But, at the same time, ASPMb, during sol–gel synthesis of which less solvent was used and which showed greater pozzolanic activity, allows concrete to retain its ability of self-cleaning without changes during the carbonation process.

4. Conclusions

Two types of anatase–silica photocatalytic materials were synthesized by the sol–gel method when the contents of solvent were different.

ASPMb, obtained with the use of a lower solvent content, is characterized by increased pozzolanic activity (1146 mg/g) due to the smaller surface coverage of diatomite particles and the higher content of Bronsted acidic sites (62.3 mmol/g). Its photocatalytic activity was 86%.

ASPMc, obtained with the use of the higher solvent content, is characterized by the more uniform distribution of anatase on the surface of diatomite and the increased photocatalytic activity of 89%. The absorption of CaO decreased to 914 mg/g; the content of Bronsted acid sites decreased to 31.5 mmol/g.

When replacing 15% of white portland cement with these additives, the acceleration in hydration of the cement system was noted. As a result of the impact of the pozzolanic activity of diatomite on the composition of the additive, there was a decrease in the content of portlandite and a formation of neoplasms with a developed morphology in cement stone.

The use of ASPMb allowed for a significant drop in the strength of cement–sand mortar to be avoided: when replacing 15% of the white portland cement, it decreased by 8.5%. In the case of ASPMc, the decrease was 14.7%.

The use of ASPMb allowed a 71% rate of self-cleaning of the cement stone surface to be provided for the removal of organic dye; this amounted to 65% in the case of ASPMc.

Fine-grained concrete containing ASPMb after forced carbonation retains the ability of self-cleaning unchanged, offering 57% rhodamine B removal or 65 h of self-cleaning from oleic acid. With the use of ASPMc, fine-grained concrete is characterized by a higher self-cleaning ability (64% or 52 h, respectively), but a lesser manifestation of the pozzolanic effect: after forced carbonation, the self-cleaning ability falls to 61% and 56 h, respectively.

References

1. Wei, Y.; Wu, Q.; Meng, H.; Zhang, Y.; Cao, C. Recent advances in photocatalytic self-cleaning performances of TiO_2-based building materials. *RSC Adv.* **2023**, *13*, 20584–20597. [CrossRef] [PubMed]
2. Haghighi, P.; Haghighat, F. TiO_2-based photocatalytic oxidation process for indoor air VOCs removal: A comprehensive review. *Build. Environ.* **2024**, *249*, 111108. [CrossRef]
3. Padmanabhan, S.K.; Pal, S.; Ul Haq, E.; Licciulli, A. Nanocrystalline TiO_2–diatomite composite catalysts: Effect of crystallization on the photocatalytic degradation of rhodamine B. *Appl. Catal. A Gen.* **2014**, *485*, 157–162. [CrossRef]
4. Zhang, G.; Liu, Y.; Hashisho, Z.; Sun, Z.; Zheng, S.; Zhong, L. Adsorption and photocatalytic degradation performances of TiO_2/diatomite composite for volatile organic compounds: Effects of key parameters. *Appl. Surf. Sci.* **2020**, *525*, 146633. [CrossRef]
5. Zuo, R.; Du, G.; Zhang, W.; Liu, L.; Liu, Y.; Mei, L.; Li, Z. Photocatalytic Degradation of Methylene Blue Using TiO_2 Impregnated Diatomite. *Adv. Mater. Sci. Eng.* **2014**, *2014*, 170148. [CrossRef]
6. Bengotni, L.; Trari, B.; Lebeau, B.; Michelin, L.; Josien, L.; Bengueddach, A.; Hamacha, R. Effect of diatomite addition on crystalline phase formation of TiO_2 and photocatalytic degradation of MDMA. *New J. Chem.* **2021**, *45*, 13463–13474. [CrossRef]
7. Bellardita, M.; Addamo, M.; Di Paola, A.; Marcì, G.; Palmisano, L.; Cassar, L.; Borsa, M. Photocatalytic activity of TiO_2/SiO_2 systems. *J. Hazard. Mater.* **2009**, *174*, 707–713. [CrossRef] [PubMed]
8. Xia, Y.; Li, F.; Jiang, Y.; Xia, M.; Xue, B.; Li, Y. Interface actions between TiO_2 and porous diatomite on the structure and photocatalytic activity of TiO_2-diatomite. *Appl. Surf. Sci.* **2014**, *303*, 290–296. [CrossRef]
9. Li, X.; Simon, U.; Bekheet, M.F.; Gurlo, A. Mineral-Supported Photocatalysts: A Review of Materials, Mechanisms and Environmental Applications. *Energies* **2022**, *15*, 5607. [CrossRef]
10. Figmig, R.; Estokova, A.; Luptak, M. Concept of Evaluation of Mineral Additives' Effect on Cement Pastes' Durability and Environmental Suitability. *Materials* **2021**, *14*, 1448. [CrossRef]
11. Yang, H.; Yang, B.; Chen, W.; Yang, J. Preparation and Photocatalytic Activities of TiO_2-Based Composite Catalysts. *Catalysts* **2022**, *12*, 1263. [CrossRef]
12. Mendoza, C.; Valle, A.; Castellote, M.; Bahamonde, A.; Faraldos, M. TiO_2 and TiO_2–SiO_2 coated cement: Comparison of mechanic and photocatalytic properties. *Appl. Catal. B Environ.* **2015**, *178*, 155–164. [CrossRef]
13. Akono, A.-T. Effect of nano-TiO_2 on C–S–H phase distribution within Portland cement paste. *J. Mater. Sci.* **2020**, *55*, 11106–11119. [CrossRef]
14. Shchelokova, E.A.; Tyukavkina, V.V.; Tsyryatyeva, A.V.; Kasikov, A.G. Synthesis and characterization of SiO_2-TiO_2 nanoparticles and their effect on the strength of self-cleaning cement composites. *Constr. Build. Mater.* **2021**, *283*, 122769. [CrossRef]
15. Cardellicchio, L. Self-cleaning and colour-preserving efficiency of photocatalytic concrete: Case study of the Jubilee Church in Rome. *Build. Res. Inf.* **2020**, *48*, 160–179. [CrossRef]
16. Şahin, O.; Bay, S.; İlcan, H.; Yıldırım, G.; Şahmaran, M. Influence of mixing methods on the NOx reduction capability and electrical properties of photocatalytic cementitious systems. *Cem. Concr. Compos.* **2021**, *115*, 103840. [CrossRef]
17. Florean, C.T.; Vermesan, H.; Thalmaier, G.; Neamtu, B.V.; Gabor, T.; Campian, C.; Hegyi, A.; Csapai, A. The Influence of TiO_2 Nanoparticles on the Physico–Mechanical and Structural Characteristics of Cementitious Materials. *Coatings* **2024**, *14*, 218. [CrossRef]
18. Hamdany, A.H.; Satyanaga, A.; Zhang, D.; Kim, Y.; Kim, J.R. Photocatalytic Cementitious Material for Eco-Efficient Construction—A Systematic Literature Review. *Appl. Sci.* **2022**, *12*, 8741. [CrossRef]
19. Kaja, A.M.; Brouwers, H.J.H.; Yu, Q.L. NOx degradation by photocatalytic mortars: The underlying role of the CH and C-S-H carbonation. *Cem. Concr. Res.* **2019**, *125*, 105805. [CrossRef]
20. Strokova, V.; Gubareva, E.; Ogurtsova, Y.; Fediuk, R.; Zhao, P.; Vatin, N.; Vasilev, Y. Obtaining and properties of a photocatalytic composite material of the "SiO_2–TiO_2" system based on various types of silica raw materials. *Nanomaterials* **2021**, *11*, 866. [CrossRef]

21.   Antonenko, M.V.; Ogurtsova, Y.N.; Strokova, V.V.; Gubareva, E.N. The effect of titanium dioxide sol stabilizer on the properties of photocatalytic composite material. *Lect. Notes Civ. Eng.* **2021**, *95*, 16–22. [CrossRef] [PubMed]

22.   Ogurtsova, Y.N.; Strokova, V.V.; Zhao, P.; Antonenko, M.V.; Gubareva, E.N. Properties of cement with photocatalytic composite material. *Mat. Sci. Forum* **2021**, *1040*, 153–158. [CrossRef]

23.   Zhang, H.; He, B.; Zhao, B.; Jm Monteiro, P. Using diatomite as a partial replacement of cement for improving the performance of recycled aggregate concrete (RAC)-Effects and mechanism. *Constr. Build. Mater.* **2023**, *385*, 131518. [CrossRef]

24.   *EN 197-1*; Cement—Part 1: Composition, Specifications and Conformity Criteria for Common Cements. European Standards: Plzen, Czech Republic, 2011.

25.   *GOST 8736*; Sand for Construction Works. Interstandard (Russia): Voronezh, Russia, 2014.

26.   *EN 196-1*; Methods of Testing Cement—Part 1: Determination of Strength. European Standards: Plzen, Czech Republic, 2016.

27.   Ogurtsova, Y.; Antonenko, M.; Gubareva, E.; Nerovnaya, S.; Strokova, V. Composition and properties of fine-grained concrete for self-cleaning coatings. *E3S Web Conf.* **2023**, *410*, 01011. [CrossRef]

28.   Black, L. *Sustainability of Construction Materials*, 2nd ed.; Woodhead Publishing: Cambridge, UK, 2016; pp. 415–457. [CrossRef]

29.   Donatello, S.; Tyrer, M.; Cheeseman, C.R. Comparison of test methods to assess pozzolanic activity. *Cem. Concr. Comp.* **2010**, *32*, 121–127. [CrossRef]

30.   Nechiporenko, A.P. *Donor-Acceptor Properties of the Surface of Solid-Phase Systems. Indicator Method*, 1st ed.; Lan: Saint-Petersburg, Russia, 2017; pp. 32–61.

31.   Nelyubova, V.V.; Sivalneva, M.N.; Bondarenko, D.O.; Baskakov, P.S. Study of activity of polydisperse mineral modifiers via unstandardized techniques. *J. Phys. Conf. Ser.* **2018**, *118*, 12029. [CrossRef]

32.   *UNI 11259*; Photocatalysis—Determination of the Photocatalytic Activity of Hidraulic Binders—Rodammina Test Method. Ente Nazionale Italiano di Unificazione (UNI): Roma, Italy, 2008.

33.   *State Standard of Russia (GOST R) 57255-2016*; Photo Catalytic Self-Cleaning Concrete. Specifications. Standartinform: Moscow, Russia, 2016.

34.   Kozlov, D.; Bavykin, D.; Savinov, E. Effect of the acidity of TiO_2 surface on its photocatalytic activity in acetone gas-phase oxidation. *Catal. Lett.* **2003**, *86*, 169–172. [CrossRef]

35.   Nikolaenko, E.A. Portland-pozzolan cement with increased strength properties. *Bull. ESSTUM* **2014**, *3*, 63–69.

36.   Ermolovich, E.A. Effect of grinding on the donor-acceptor properties of surfaces of backfill mix components. *J. Min. Sci.* **2013**, *49*, 839–846. [CrossRef]

37.   Zakharova, N.V.; Sychev, M.M.; Korsakov, V.G.; Myakin, S.V. Evolution of donor-acceptor centers on the surface of $BaTiO_3$—$CaSnO_3$ ferroelectric materials in the course of their dispersion. *Condens. Matter Interphases* **2011**, *13*, 56–62.

38.   Taylor, H.F.W. *Cement Chemistry*, 2nd ed.; Thomas Telford Publishing: London, UK, 1997; pp. 212–214.

39.   Lawrence, P.; Cyr, M.; Ringot, E. Mineral admixtures in mortars: Effect of inert materials on short-term hydration. *Cem. Concr. Res.* **2003**, *33*, 1939–1947. [CrossRef]

40.   Ivanov, I.M.; Matveev, D.V.; Orlov, A.A.; Kramar, L.I. Influence of water-cement ratio and superplasticizers on the heat release, cement hydration and hardening processes. *Bull. South Ural. State Univ. Ser. Constr. Eng. Archit.* **2017**, *17*, 42–49.